Practice of Mechanics Experiment Teaching Aimed at Solving Students' Problem Based on Simulation Technology in Higher Vocational Colleges

Shixia Lv, Shang Wang(✉), and Xuelei Wang

School of Automotive Engineering, Beijing Polytechnic, Liangshuihe 1st Street of Economic and Technological Development Zone, Beijing, China
wangshang@bpi.edu.cn

Abstract. The main employment positions of students in vocational colleges are technical operation positions in enterprise production lines. In addition to theoretical knowledge, the cultivation of students' ability to identify problems, ask questions and analyze problems is important for their future work. In this paper, we use finite element modeling and simulation technology to solve students' doubts about mechanics experiments. In the process of solving the confusion, the research team involved the students in the whole process of modeling and simulation in the form of task assignment and seminar. The results of the teaching practice showed that: (1) the finite element modeling and simulation can obtain the Mises stress nephograms that can clearly show the stress and deformation of the specimen, which solved the students' doubts; (2) students have a deeper understanding of mechanical experiments by completing the task of structural dimensioning before modeling; (3) the students' data processing skills and text expression skills were exercised by completing the task of data analysis after the simulation. The use of finite element simulation technology to solve students' learning problems is an important innovation in vocational education teaching methods.

Keywords: mechanics experiment teaching · simulation technology · students' problem · vocational colleges

1 Introduction

Vocational education and general education are two different types of education with equal importance. Since the reform and opening up, vocational education has provided strong talent support for China's economic and social development. As China enters a new development stage, industrial upgrading and economic structure adjustment are accelerating, and the demand for technical and skilled talents in all walks of life is becoming more and more urgent; therefore, the important position and role of vocational education are becoming more and more prominent [4].

China has the most complete industrial system in the world. To push forward the upgrading of manufacturing industry and the development of emerging industries and

Z. Zhan et al. (Eds.): ICBDIE 2022, AHCS 5, pp. 205–218, 2023.
https://doi.org/10.2991/978-94-6463-034-3_21

Fig. 1. Teaching site of tensile experiment of material mechanics.

promote industrial development from medium and low-end to medium and high-end, there is an urgent need for a large number of highly skilled talents [1]. However, at present, the total number of highly skilled talents is only more than 50 million in China, accounting for only 28% of the total number of skilled talents, while that in developed countries is generally more than 40%. It is estimated that by 2025, there will be a demand gap of nearly 30 million high skilled talents in the top ten key fields of China's manufacturing industry [11]. The cultivation of skilled and applied talents is inseparable from scientific teaching methods and the reform of teaching methods is the top priority of vocational education [6]. New generation technologies, such as Internet and virtual simulation, should be explored and applied to improve teaching quality by teachers in vocational colleges.

Material Mechanics is not only a required course for engineering majors such as machinery, automobile and rail transit, but also an important basic course of many specialties. The learning effect of Material Mechanics will directly affect follow-up related professional courses, such as mechanical design, hydraulic and transmission, metal cutting, automobile manufacturing technology. Because the course content is numerous and difficult, and many theorems and formulas need complex mathematical derivation process, students generally feel great academic pressure and have no interest in learning [7]. The mechanics experimental part of Material Mechanics has long been a weak link in the teaching of higher vocational colleges [8].

Take the torsion experiment as an example. In most cases, there is only one teacher who can only operate one device for experiments. Considering the danger of the experiment, the teacher will not let students observe the sample closely. Therefore, the change of sample size, especially the process of axial deformation and stress distribution can only be observed clearly by three or four students in a class with dozens of students, as shown in Fig. 1. Some vocational colleges are worried about safety accidents and even cancel all mechanics experimental teachings.

In order to improve students' interest in learning, teachers often introduce engineering cases in class and encourage students to discuss them. Students often ask specific questions. Many problems need to be determined by mechanical experiments. The solution of these problems is facing challenges. For example, the school has no relevant experimental equipment. Some tests are dangerous, and students are not allowed to do

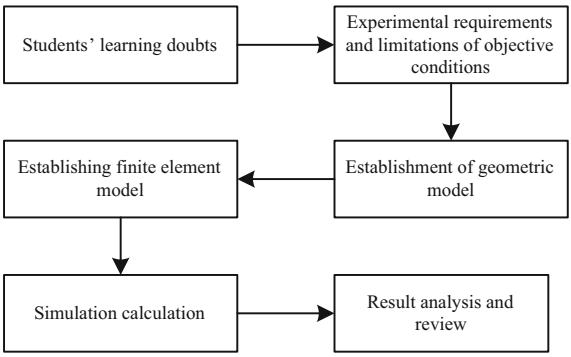

Fig. 2. The research logic diagram of this paper.

relevant experiments. Despite many challenges, students' learning problems should be paid enough attention, and teachers should find ways to solve them.

With the improvement in computing ability of computers and the popularization of simulation software, simulation technology has been greatly developed in many fields, such as transportation [3], fire protection [9], medical treatment [5], metallurgy [12], military [10], and education [2]. It is feasible to use simulation technology to solve the doubts of students in mechanics experiment teaching.

This paper has made an attempt and achieved good teaching results. The logical structure of this paper is shown in Fig. 2.

2 Students' Doubts

After performing tensile mechanics experiments, several students became interested in the fracture behavior of the specimens. The students believed that the forces in the middle of the specimen and the sides of the specimen were different. The core has metal all around it, while the edge has metal only on the side pointing to the center. Because the forces are different, the time to fracture should be different. However, this phenomenon was not observed when the mechanics experiment was performed. The students told the research team about their doubts.

The research team confirmed the students' guess and told them about the fracture process: the core fractured first and the sides fractured later. The students then looked up tensile experiments on the Internet and found that many specimens were not cylindrical as used in teaching, but rectangular specimens.

The students wanted to do tensile experiments on rectangular specimens to observe the core and edge fracture behavior.

The research team confirmed the students' experimental needs, but the school does not currently have the experimental conditions to perform tensile tests on rectangular specimens. On the one hand, the school does not have rectangular specimens. On the other hand, even if the steel plates were purchased, the school did not have a wire cutting device to cut them into tensile specimens.

In order to solve the learning problem raised by the students and to increase their motivation, the research team decided to use finite element modeling and simulation to obtain the tensile damage stress nephogram of the rectangular specimen.

Before finite element modeling, detailed model data and simulation requirements were needed. Under the guidance of the research team, the students completed these work tasks.

3 Modeling

In order to exercise the students' problem analysis skills, the research team asked the students to consult the literature online to design the specific dimensions of the specimen and draw a 3D drawing using Solidworks software. In addition, the research team asked the students to specify the data that needed to be calculated for the simulation. These tasks were required to be compiled by the students into a paper version of the report.

3.1 Geometric Model

The structure of standard tensile sample is shown in Fig. 3. The sample includes a test part in the middle and two clamping parts at both ends. The test part is used to measure the stress/strain of the sample; the clamping parts are used for clamping and applying tensile force to the sample by the experimental device.

The geometric model of the specimen drawn by the students is shown in Fig. 2. The central rectangle is the test section. The dimensions of the test section are: length $L =$ 100 mm (X-axis direction), width $B = 20$ mm (Y-axis direction) and thickness $H =$ 5 mm (Z-axis direction). The dimensions of the two clamping parts are identical. There is a symmetrical chamfer between the test part and the clamping part, as shown in Fig. 3. The diameter of the chamfer is 5 mm and the angle is 90°. The clamping part has a length of 30 mm in the X-axis direction, a total length of 30 mm in the Y-axis direction and a thickness of 5 mm (equal to the test part). The test object is mild steel. The experimental parameters required by the students are as follows:

The stretching speed of the experimental device is $v = 1$ mm/s, and the stretching time is $t = 15$ s.

The experimental data to be measured by the students are as follows:

(1) the time to fracture of the core in tension and the Mises stress nephogram at the time of core cracking.

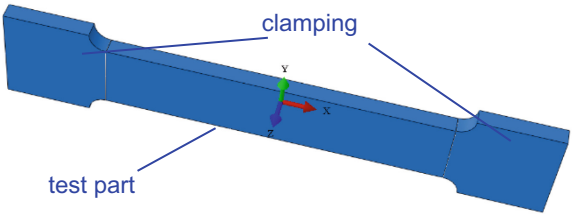

Fig. 3. Structure of tensile specimen with rectangular section.

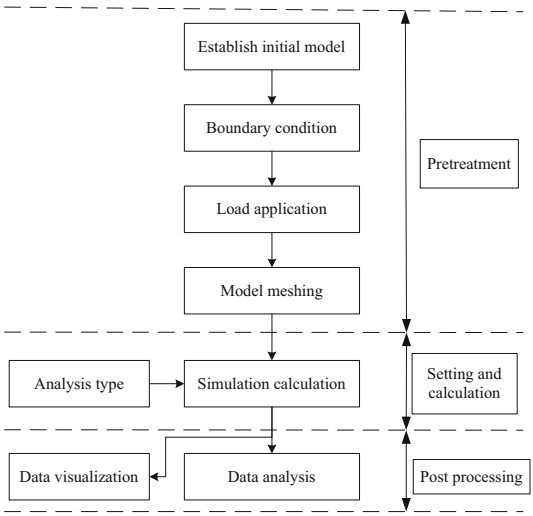

Fig. 4. The steps of ABAQUS modeling and simulation.

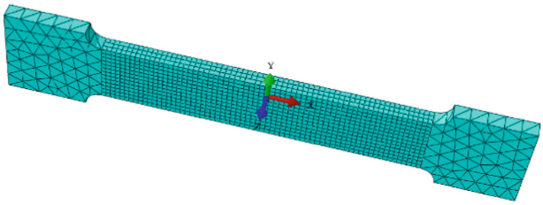

Fig. 5. Finite element model after meshing.

(2) the time to complete fracture of the specimen, and the Mises stress nephogram after fracture.

3.2 Finite Element Modeling

According to the geometric dimensions provided by the students, the 3D finite element model was established with ABAQUS software. The modeling and simulation calculation process of this paper is shown in Fig. 4.

The model consists of three parts. Two clapping parts are symmetrical. Considering that deformation of the two clapping parts are very small, and has a little effect on the experimental results, they are set as a rigid body in the finite element model. The element type of the two clapping parts are chosen as C3D10M, and the grid cell size is set to 5 mm.

Setting of material property of the test part: density of the material $\rho = 7.9 \times 10^3$ kg/m^3, elastic modulus $E = 210$ GPa, and Poisson's ratio $\lambda = 0.3$. In order to better simulate the necking and fracture of the sample, set fracture strain value $\varepsilon_0 = 1.4$ and failure display value $x_0 = 0.04$. The element type of finite element model is chosen as C3D8R, and the grid cell size is set to 1.5 mm.

The "tie" command is used for adhesion between the two clapping parts and the test part. Special points RP-1 (- 90, 0, 2.5) and RP-2 (90, 0, 2.5) are set to facilitate the loading of the force/displacement of the model. The point RP-1 is bound to the left clapping part through the "couple" command, and the point RP-2 is bound to the right clapping part through the "couple" command. The finite element model after meshing is shown in Fig. 5. The constraint of finite element is set as six degrees of freedom full constraint on the point RP-1. Apply velocity to the point RP-2. The direction of speed is X-axis negative direction, and the size of speed $v = 1$ mm/s. The time of the "Step" command is set to $t = 15$ s, and the "H-output" command is set to $T = 20$ times.

4 Model Simulation

4.1 Initial Stress Nephogram

The model conducted calculations on a computer. Figure 6 shows the Mises stress nephogram of the finite element model at different moments when there is no obvious necking.

It can be seen from Fig. 6, as time goes on, stress concentration gradually appears in the middle of the sample. Figure 6 (a) is the Mises stress nephogram of the finite element model when $t = 0.75$ s, at which there is almost no necking phenomenon. The stress in the nephogram diagram is uniform, and the maximum Mises stress is 587.7 MPa.

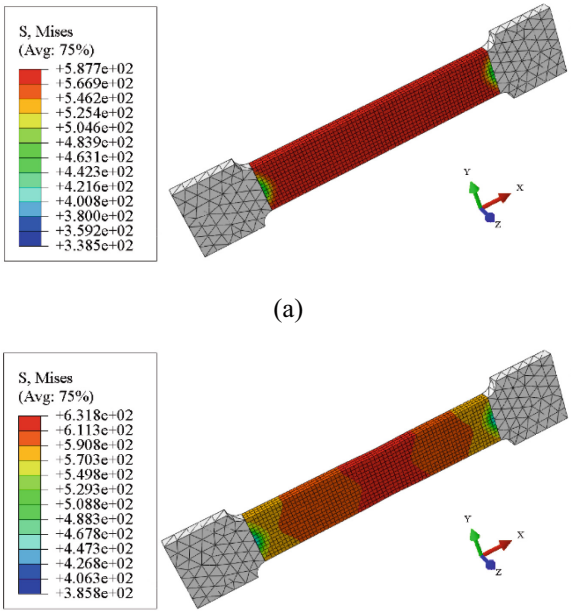

Fig. 6. Mises stress nephograms at different times: (a) t = 0.75 s; (b) t = 3.75 s.

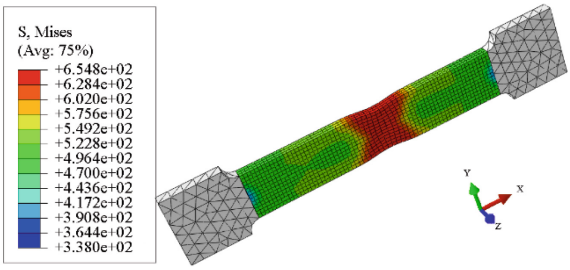

(a)

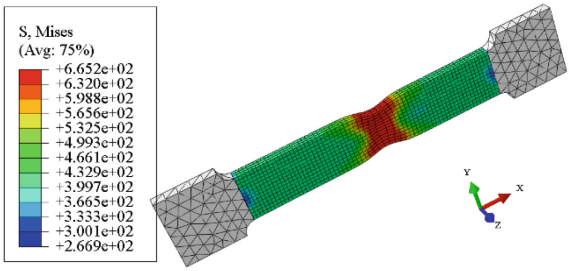

(b)

Fig. 7. Mises stress nephograms at different times: (a) t = 6 s; (b) t = 8.25 s.

Figure 6 (b) is the Mises stress nephogram of the finite element model when $t = 3.75$ s. Compared with Fig. 6 (a), the stress distribution of the model is obviously uneven, and extremely slight necking began to appear. The stress/strain in the middle of the sample is greater than that on both sides, and the maximum Mises stress is 631.8 MPa.

The necking phenomenon of the sample becomes more and more obvious with time. Figure 7 shows the Mises stress nephogram of the finite element model at different moments when necking is obvious.

Figure 7 (a) is the Mises stress nephogram of the finite element model when $t = 6$ s, at which there is an obvious necking phenomenon. The stress/strain in the middle of the sample is greater than that on both sides, and the maximum Mises stress is 654.8 MPa. Different from Fig. 6 (a) and Fig. 6 (b), Fig. 7 (a) shows a larger difference between the maximum Mises stress and the minimum Mises stress of the finite element model. This is because necking releases energy and large-scale plastic strain weakens strain values on both sides of the sample, resulting in a certain reduction in the stress at both ends.

Figure 7 (b) is the Mises stress nephogram of the finite element model when $t = 8.25$ s, at which the necking phenomenon is very obvious. At this time, the stress concentration of the model is more obvious (at the necking position). However, the maximum Mises stress changes little, and its value is 665.2 MPa. The plastic flow of metal caused by necking hinders the increase of stress.

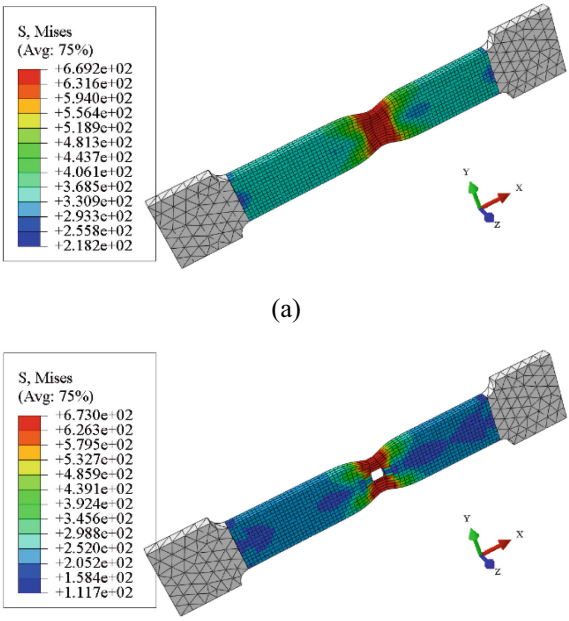

Fig. 8. Mises stress nephograms at different times: (a) t = 0.75 s; (b) t = 3.75 s.

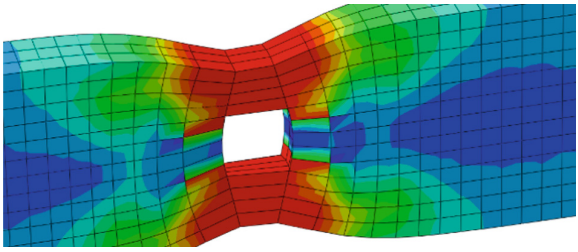

Fig. 9. Microscopic observation of fracture at t = 10.5 s.

4.2 Fracture Process of Specimen

Figure 8 shows the fracture process of the sample. Figure 8 (a) is the model stress nephogram before fracture. As can be seen from Fig. 8 (a), the necking phenomenon is close to the limit, and the elements in the middle of necking are greatly elongated. At this time, the maximum Mises stress of the finite element model is 669.2 MPa.

Subsequently, the fracture of the specimen begins. As can be seen from Fig. 8 (b), the 4 elements in the center of the necking part reach the strain limit set by the model and are deleted from the finite element model. At this time, the maximum Mises stress of the finite element model is 673.0 MPa. The finite element model uses the continuous deletion of elements to simulate the fracture phenomenon of samples. According to the

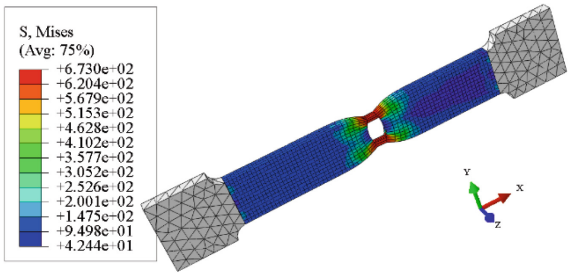

(a)

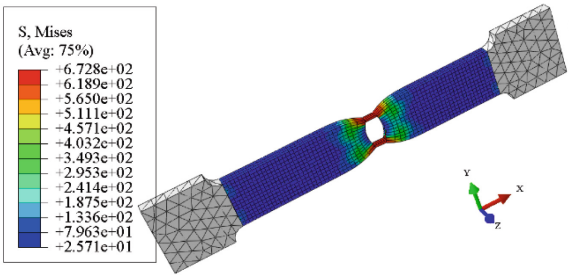

(b)

Fig. 10. Mises stress nephograms at different times: (a) t = 12 s; (b) t = 12.75 s.

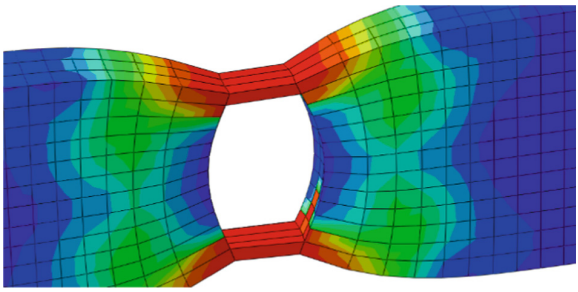

Fig. 11. Microscopic observation of the sample fracture at t = 12.75 s.

setting of material properties, the deleted element has reached the fracture threshold. Obviously, the results of finite element model simulation verify the students' conjecture.

In order to analyze the fracture law, microscopic observation was carried out at the fracture, as shown in Fig. 9. It can be seen from Fig. 9 that the stress of the unit around the fracture is released along the X-axis direction. Along the Y-axis direction, the elements that have not been broken bear the additional tension of the deleted elements, so the stress and strain are large.

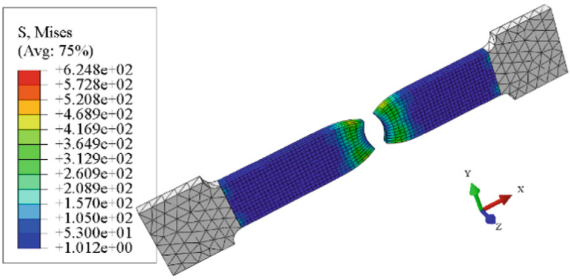

Fig. 12. Mises stress nephograms at t = 13.5 s.

As time goes on, more and more elements are deleted under the action of tension. Figure 10 (a) is the Mises stress nephogram of the finite element model with $t = 12$ s, the maximum Mises stress of the finite element model is 673.2 MPa.

It can be seen from Fig. 10 (a), as time goes on, more elements in the center of the necking part reach the strain limit set by the model and are deleted from the finite element model. Figure 10 (b) is the Mises stress nephogram of the finite element model with $t = 12.75$ s, the maximum Mises stress of the finite element model is 672.8 MPa. At this time, there are only a few elements at the edge of the fracture location. Figure 11 is the microscopic observation diagram at the fracture with $t = 12.75$ s. As can be seen from Fig. 11, the edge elements are pulled very long in the X-axis direction under external tension. In addition, the elements at the edges are moving towards the center (X-axis), which is much distorted. Subsequently, the sample has been completely broken, as shown in Fig. 12.

After the specimen is pulled, the stress of a large number of elements at the fracture is released. The maximum Mises stress value was 624.8 MPa, and the maximum Mises stress occurred at the fracture surface. Large-scale plastic deformation has occurred at the fracture of the sample, which cannot be restored.

The Mises stress nephograms above solved the students' doubts perfectly. Here is a summary of the experimental results that the students need, as follows:

The fracture time of the sample core is $t = 10.5$ s; the total tensile displacement is $s = 10.5$ mm. Mises stress nephogram during core cracking is shown in Fig. 8 (b).

The complete fracture time of the sample is $t = 13.5$ s; the total tensile displacement is $s = 13.5$ mm. Mises stress nephogram at complete fracture is shown in Fig. 12.

4.3 Statistics of Maximum Mises Stress

The maximum Mises stress at different times was calculated by invoking the data in ODB, and the statistical results shown in Fig. 13 was obtained.

It can be seen from Fig. 13 that the maximum Mises stress of the model increased with time before the specimen fracture. The maximum Mises stress increased significantly at the initial stage of stretching. When the maximum Mises stress reached 650 MPa, the increase rate began to slow down.

This is because large scale plastic deformation begins to occur at the necking. The maximum Mises stress hardly changed with time when it reached 670 MPa. When the

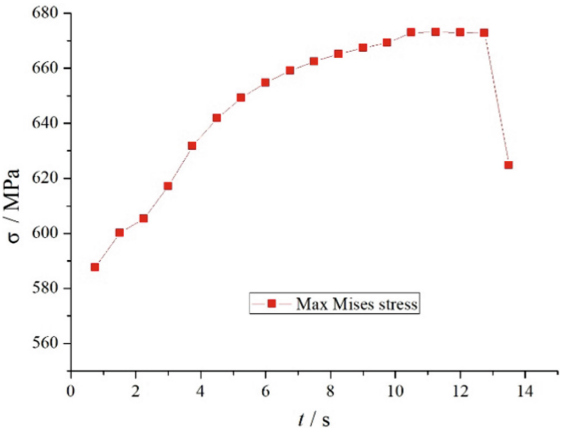

Fig. 13. Maximum Mises stress statistics.

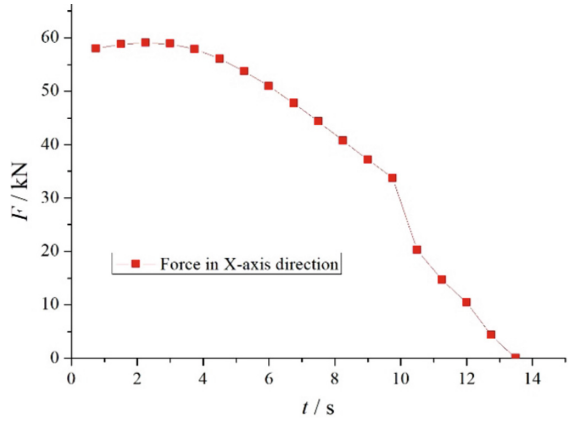

Fig. 14. Statistics of tension value in X-axis direction.

specimen was completely fractured ($t = 13.5$ s), the maximum Mises stress directly drops from 672.8 MPa to 624.8 MPa.

4.4 Variation Law of Tensile Force

The model ODB data is called to make statistics on the tension values along the X-axis at different times. The statistical results are shown in Fig. 14.

As can be seen from Fig. 14, the tensile force applied to the sample first increases slowly and then decreases with time. This evolution law is consistent with the Mises nephogram map in Fig. 6, Fig. 7, Fig. 8 and Fig. 10 above. It can be seen from Fig. 14 that the tensile force applied on the sample at the beginning is already very large, with a value of 57.98 kN. Because students mainly want to study necking and fracture behavior, the tensile speed set in the model is relatively large. When $t = 2.25$ s, the tensile force

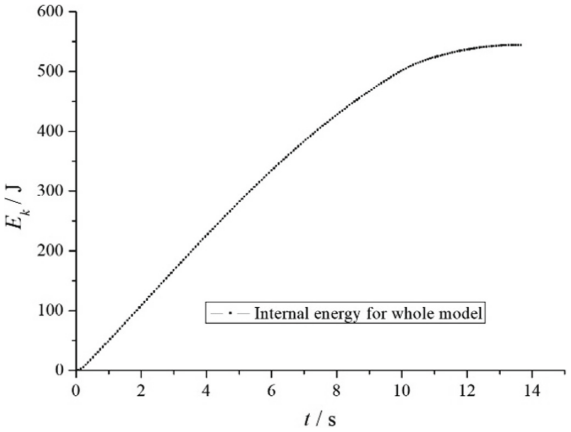

Fig. 15. Statistics of internal energy at different time.

reaches the maximum value, which is 59.04 kN. The subsequent decrease in the tension value is due to the obvious plastic deformation of the metal. The necking of the sample has occurred and is becoming more and more obvious. When $t = 10.5$ s, the tension value decreases significantly. The tension drops from 33.73 kN to 20.25 kN. This is due to the fracture in the center of the necking area (refer to Fig. 8 and Fig. 9). The whole fracture process lasted until $t = 13.5$ s. At this point, the sample is completely broken and the tensile value becomes zero.

4.5 Variation Law of Internal Force

The ODB data of the model is called, and the internal energy value of the sample is counted. Figure 15 shows the change law of strain energy of the whole finite element model over time.

It can be seen from Fig. 15 that in the initial stage, under the action of loading on the point RP-1, strain energy increases rapidly. When $t = 10$ s, the value of strain energy is 503.1 J. With the increase of time, the subsequent increase of internal energy began to become slow. After $t = 13.2$ s, the internal energy hardly changes, and the value fluctuates slightly between 544.2 J and 544.4 J, because the sample has been completely broken.

As mentioned above, the statistics of the maximum Mises stress value enables students to have a deeper understanding of the law of stress evolution. The statistics of the tension value in the X-axis direction gave the students a deeper understanding of the evolution law of external load. The statistics of internal energy values enable students to have a deeper understanding of the accumulation law of internal energy of the sample. These statistical data are consistent with the Mises stress nephogram mentioned above.

In short, finite element modeling and simulation perfectly solved the students' learning doubts. Moreover, in the process of modeling and simulation, students have done a lot of work, and their abilities have also been trained and improved.

5 Result

As mentioned in the previous section, the finite element simulations yielded a large amount of data and Mises stress nephograms. These data and stress nephograms solved the students' learning doubts and gave them a better understanding of the tensile experiments.

Based on this, a detailed test report was compiled by the students at the request of the research team. This test report, signed by the participating students, was printed and distributed to several classes as reading material for the students after school. These students were significantly more motivated to learn because the fruits of their work were studied by everyone.

6 Conclusion

The students have encountered problems in the study of mechanical experiments, and hope to verify them by doing experiments. However, the school does not have relevant instruments and test samples. Enough attention should be paid to the solution of students' learning problems. The research team put forward a method of using finite element modeling and simulation calculation to obtain materials such as pictures, animation, so as to solve the students' doubts. In the process of raising, analyzing and solving problems, students' abilities in all aspects have also been exercised and improved. The main conclusions of this paper include:

(1) The model simulation obtains clear demonstration animations, which can repeatedly show necking and fracture of the sample under external load. The Mises stress data at different moments are obtained by model simulation and displayed in different color forms (the more red, the greater the stress data); these materials obviously enhance students' interest in learning and expand the students' knowledge.
(2) The questions raised by students in their study should be taken seriously by teachers. The method of finite element simulation can be considered, when there is no experimental equipment in the school. More new technologies and ideas should be tried and applied in vocational colleges. The reform of teaching methods should be student-centered. The research idea of this paper should be applied to more fields of vocational education.

Acknowledgements. The research of this paper is supported by the Project of Beijing Office for Education Sciences Planning (Grant No. CCDB2020135 and No. CGDB21208), and the Project of China Vocational Education Association (Grant No. ZJS2022YB024).

References

1. Jin Y. (1993). Technical and vocational education in the People's Republic of China: current status and prospects. J. The Vocational Aspect of Education, 45(2): 135-143.
2. Koźlak M, Nawrat A, Kurzeja A. (2014). Virtual reality simulation technology for military and industry skill improvement and training programs. J. Szybkobieżne Pojazdy Gąsienicowe, 2 (35): 5-12.
3. Nguyen Q T, Bouju A, Estraillier P. (2012). Multi-agent architecture with space-time components for the simulation of urban transportation systems. J. Procedia-Social and Behavioral Sciences, 54: 365-374.
4. Shi W. (2013). Issues and problems in the current development of vocational education in China. J. Chinese Education & Society, 46(4): 12-21.
5. Spooner N, Hurst S, Khadra M. (2012). Medical simulation technology: educational overview, industry leaders, and what's missing. J. Hospital topics, 90(3): 57-64.
6. Wang L, Jiang D. (2013). Chinese vocational education: borrowing and reforming: an interview with professor dayuan jiang, MOE research fellow. J. Chinese Education & Society, 46(4): 92-99.
7. Wang S, Ma J, Liu H, et al. (2021). Exploration on teaching practice of material mechanics course for the run-through external cultivation in vocational college[C]//2021 4th International Conference on Humanities Education and Social Sciences (ICHESS 2021). Atlantis Press, 1406–1410.
8. Wang T, Luo H F, Wang J, et al. (2016). Exploration and practice of material mechanics teaching reform. J. Experimental Science and Technology, 14(3): 116-118.
9. Wei Z. (2012). Application of computer simulation technology [CST] in buildings' performance-based fire protection design. J. Procedia Engineering, 37: 25-30.
10. Wilton D. (2001). The application of simulation technology to military command and control decision support[C]//SimTect 2001 Conference Proceedings, 9–14.
11. Wu X, Ye Y. (2018). An introduction to technical and vocational education in China. J. Technical and Vocational Education in China. Springer, Singapore, 1–43.
12. Xu T, Song G, Yang Y, et al. (2021). Visualization and simulation of steel metallurgy processes. J. International Journal of Minerals, Metallurgy and Materials, 28(8): 1387-1396.